Available online at www.sciencedirect.com
ScienceDirect
Trans. Nonferrous Met. Soc. China 25(2015) 838−843
Transactions of Nonferrous Metals Society of China
www.tnmsc.cn

DSC analysis of commercial Cu−Cr−Zr alloy processed by equal channel angular pressing

K. ABIB, F. HADJ LARBI, L. RABAHI, B. ALILI, D. BRADAI

Faculty of Physics, University of Sciences and Technology Houari Boumediene,
BP 32 El Alia, Bab Ezzouar, Algiers, Algeria

Received 22 March 2014; accepted 14 August 2014

Abstract: Samples of a commercial Cu−1Cr−0.1Zr (mass fraction, %) alloy were subjected to equal channel angular pressing (ECAP) up to 16 passes at room temperature following route Bc. Differential scanning calorimetry (DSC) was used to highlight the precipitation sequence and to calculate the stored energy, recrystallization temperature and activation energy after each ECAP pass. On another hand, electrical properties were correlated with the dislocation density. Results show that the stored energy increases upon increasing ECAP pass numbers, while the recrystallization temperature decreases significantly.

Key words: equal channel angular pressing (ECAP); Cu−Cr−Zr alloy; differential scanning calorimetry (DSC); electrical conductivity; stored energy

1 Introduction

Cu−Cr−Zr alloys attracted growing interests in electric/microelectronics areas and nuclear fusion reactors [1]. These alloys are known to be strengthened by conventional cold working, as well as by precipitation of Cr and complex Cu−Zr phases [1−3]. As long as severe plastic deformation processing was capable of producing strong materials with good ductility, these techniques were also applied to Cu−Cr−Zr alloys [4]. Since the work of VINOGRADOV et al [5] associated with thermal stability after SPD processing of Cu−Cr−Zr, very little work was devoted to highlight the thermodynamic aspects associated with thermal energy (enthalpy changes) that may lead to the improved knowledge of the chemical and microstructural changes that occur during and/or after SPD processing [6].

The mechanical properties such as strength and ductility of Cu−Cr−Zr have been been considerably optimized by combining severe plastic deformation and precipitation [7].

Moreover, serious controversies still exist on the sequence and nature of precipitates that can appear during annealing after conventionally or severely deformed Cu−Cr−Zr alloy [5,7,8].

The present work aims to evaluate some thermodynamics (stored energy) and kinetics (temperature and activation enthalpy) of recrystallization as well as to clarify the sequence of precipitation after ECAP processing of a Cu−1Cr−0.1Zr alloy.

2 Experimental

The material considered in this work is a Cu−1Cr−0.1Zr alloy that was supplied in the form of rod bars by Goodfellow. Billets of 10 mm in diameter and 60 mm in length were then machined for ECAP processing and solution heat-treated for 1 h at 1040 ºC in a protective inert gas atmosphere followed by a subsequent water quenching. The billets were processed by ECAP at room temperature up to 16 passes using route B_c (sample rotation of 90° along their longitudinal axis in the same direction after each pass). The ECAP die used in these experiments had an internal angle of Φ=90° and an outer arc of curvature of ψ=37°. The samples were coated with molykote spray and deformed at a constant cross head speed of 0.02 m/s.

In order to clarify the precipitation sequence and estimate the stored energy and the recrystallization temperature, miniature specimens of 40−50 mg were cut near the axial centre of the as-pressed billets and subjected to DSC analysis using a Labsys Evo (1600 °C) facility under a constant heating rate of 10, 20, 30 and

Corresponding author: B. ALILI; Tel: +213-550-282-565; Fax: +213-21-247-344; E-mail: alili.baya@yahoo.fr
DOI: 10.1016/S1003-6326(15)63671-8

40 °C/min in argon atmosphere. The DSC scanning temperature ranged from 30 to 700 °C and at least three specimens were probed for each heating rate. Standard Al_2O_3 samples were thermally scanned to calibrate the calorimeter prior to measurement and to obtain a baseline.

The activation energy of precipitation and recrystallization was calculated for the material processed for 1, 8 and 16 passes based on DSC measurements at heating rates of 10, 20, 30 and 40 °C/min. The dependence of the peak temperature on the heating rate was used to calculate the apparent activation energy for recrystallization based on the KISSINGER's method [9] given by

$$\ln\left(\frac{v}{t_{\mathrm{p}}^{2}}\right)=A-\frac{\Delta G}{RT_{\mathrm{p}}} \tag{1}$$

where v is the heating rate, t_{p} is the peak temperature, A is a constant, G is the apparent activation energy and R is the gas constant.

An X-ray diffraction profile analysis for each sample was carried out from the flat and polished surface by Brukers D8 Advance X-ray diffractometer using Cu K_{α} radiation operated at 40 kV and 20 mA. The 2θ Bragg angle varied from 30° to 88°. The step scan was 0.02° and the counting time per step was 7 s. Electrical conductivity measurements were performed ex situ using a four probe set-up (DFP-Research Model from SVSLabs).

The formation enthalpy of Cu clusters, Cu_5Zr and $Cu_{51}Zr_{14}$ precipitating phases were calculated within the framework of density functional theory (DFT) using pseudopotential method as implemented in the pseudo-potential plane wave self-consistent field package (Quantum Esspresso) [10]. The many-body problem of interacting electrons and nuclei was mapped to a series of one-electron equations in the so-called Kohn-Sham (KS) equations [11,12]. The generalized gradient approximation (GGA) of PERDEW et al (PBE) [13] of the local density approximation was considered to include the exchange-correlation energy and ultrasoft pseudopotentials of VANDERBILT [14] were used. A well converged value of the cut-off energy and the k-point mesh over the Brillouin zone were considered for both the structure of both compounds. All systems were allowed to fully relax using Broyden-Fletcher-Goldforb-Shanno (BFGS) scheme [15] until the total energy has converged to less than 10^{-5} eV/atom, the maximum force has converged to lower than 0.004 eV/Å and the maximum displacement was 0.002 Å.

3 Results and discussion

Figure 1 presents a compilation of DSC scans showing the enthalpy release during linear heating at 20 °C/min of the ultra-fine grained Cu−1Cr−0.1Zr alloy subjected to 1, 4, 8 and 16 ECAP passes. Other scans (not shown here) corresponding to 10, 30 and 40 °C/min exhibit almost the same trends.

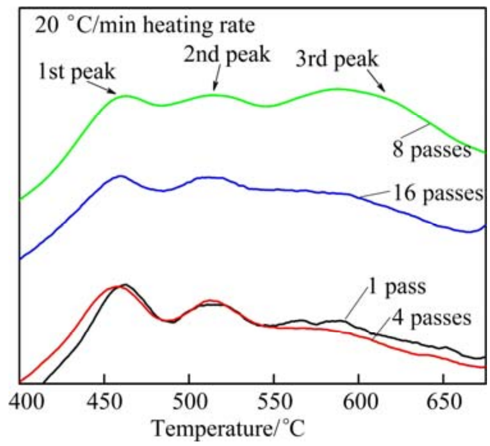

Fig. 1 Enthalpy release rate during linear heating of ultra-fine grained Cu−1Cr−0.1Zr alloy subjected to 1, 4, 8 and 16 ECAP passes

From Fig. 1, the third DSC peak near 600 °C and corresponding to recrystallization is more resolved for scans after 8 passes than for 1, 4 and 16 passes. The preceding peaks around (1st and 2nd peaks) confirm the complex precipitation sequence already mentioned in Ref. [5]. The first two peaks can be associated with Cr clustering and Cu_3Zr (replaced by $Cu_{51}Zr_{14}$ [16]) precipitation, respectively. All the peaks are however slightly shifted towards higher temperatures upon straining. It is worth mentioning that some DSC scans associated with recrystallization exhibit more than one peak (at least two, as shown in Fig. 1 after 1 ECAP pass). The occurrence of multiple peaks, within the recrystallization one, has already been observed in Al−Mg alloy after ECAP processing where the two present peaks are associated with the advent (recovery process) and the completion of the recrystallization process, while only one single peak appears in the cold-rolled alloy and that is related to the completion of the recrystallization [17]. However, the microstructures existing in the two alloys are somewhat different. The Al−Mg alloy after ECAP processing and dynamic aging exhibits a duplex microstructure divisible into areas of unrecrystallized grains and areas where recrystallization is essentially complete [17]. In the present work, the Cu−1Cr−0.1Zr alloy may exhibit a quite different microstructure consisting of not only duplex microstructure as observed above but also fine Cr and $Cr_{51}Zr_{14}$ precipitations [5,16], which interact with recrystallization, resulting in a rather very complex DSC signal.

An attempt has been made to characterize the precipitated phases through X-ray diffraction (XRD) analysis. Several XRD patterns are recorded for Cu−1Cr−0.1Zr alloy samples after full DSC scans. Unfortunately, as shown in Fig. 2, for a sample alloy after DSC scan at 20 °C/min after ECAP processing up to 8 passes, no trace of definite peak associated with any precipitated phase could be depicted from the pattern and only Cu (matrix) peak is presented. The fine Cr and $Cr_{51}Zr_{14}$ precipitates result in DRX peak signals that are fully masqued by the background and then only an in situ high energy synchrotron diffraction analysis should substantially reveal these peaks as shown in a recent study [18]. Resulting DSC scans may be interpreted in terms of interactions between precipitation and recrystallization. During dynamic annealing (DSC), the ECAPed alloy samples manifest a delayed process of recrystallization until the whole complex panel of precipitation occurs. Similar observations are reported in Al−Mg−Si alloy where a small addition of Sc suppresses the recrystallization and retains the ultrafine grained structure to temperatures exceeding 450 °C [19,20]. However, the shift of the recrystallization peak towards lower temperatures as observed by these authors [19,20] is not observed in the presently studied Cu−1Cr−0.1Zr alloy. Their interpretation based on the fact that SPD processing may induce changes in the precipitation kinetics through the modification of the effective diffusivity and the density of nucleation sites for precipitation could not be applied in the present case because of the so complex modes of precipitation.

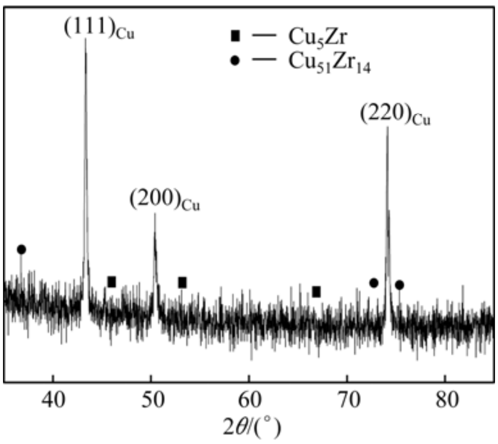

Fig. 2 XRD pattern of Cu−1Cr−0.1Zr alloy after DSC scan at 20 °C/min after ECAP processing up to 8 passes

Similar delay of the recrystallization temperature was also observed in a Cu−Cr−Zr alloy after conventional deformation by rolling [21,22]. These authors discussed the overall effect of the Cr particle clusters retarding the recrystallization with a special emphasis to their size distribution. They have estimated the pinning force that the particles may produce per unit area from the Zener equation [23] given by

$$F_{\max} = \frac{3 f_{\mathrm{v}} \sigma_{\mathrm{gb}}}{2r} \tag{2}$$

where f_v is the volume fraction of particles, σ_{gb} is the interface energy per unit area and r is the particle radius. The calculated values associated with the presence of fine Cr particles (average diameter of 15 nm and interparticle spacing of 80 nm) confirm the strong pinning force (four times larger than that for large particles with average diameter of 0.85 μm and interparticle spacing of 2.8 μm) exerted on moving boundaries. Nanoscale precipitation of Cu_5Zr was evidenced by SUN et al [24] while larger $Cu_{51}Zr_{14}$ precipitates (up to 100 nm) were observed by HUANG et al [2] in Cu−Cr−Zr alloys. $Cu_{51}Zr_{14}$ precipitates did not contribute to the overall hardening of the alloy as the tiny Cr precipitates ones did. Their effect on recrystallization should also not be significative since the critical particle size to promote recrystallization within the deformation zone around particles was 2.5−3 μm [22].

A controversial estimation of the formation enthalpy of Cu_5Zr and $Cu_{51}Zr_{14}$ phases using a CALPHAD (−10.3/−12.9 kJ/mol) and ab initio approaches (−12.5/−8.6 kJ/mol) [25] and present work (−12.23/ −5.484 kJ/mol) exists. It is difficult to draw any definitive conclusion about their relative stability. The $Cu_{51}Zr_{14}$ phase could be more stable because ab initio estimations are performed at 0 K and the consideration of a probable temperature effect should correct the obtained values. GOSH et al [25] reported from experimental observations [26,27] that both phases were known to be stable down to at least 773 K.

The activate energy of Cr clustering and the nano precipitation of $Cu_{51}Zr_{14}$ phase estimated from Kissinger plots for samples processed up to 1, 8 and 16 ECAP passes ranged between 121−142 and 131−181 kJ/mol, respectively. These values fall quite good within tabulated ranges of data for Cu-based alloys [28,29]. The activation energy associated with the different phases involved is lower than the activation energy for Cr and Zr diffusion in copper. The complex precipitation process is governed by diffusion that can only proceed via a vacancy mechanism and, quiet rightly, considerable amounts of excess vacancies are evidenced in severely deformed alloys [6,30].

The stored energy has been estimated by integrating the peaks associated with recrystallization in the DSC scans. Figure 3 shows the evolution of the stored energy for recrystallization upon increasing ECAP pass number. It is obvious that it increases upon increasing strain as already reported in the literature for copper and its alloys [31−33] and saturates 0.7−0.8 J/g.

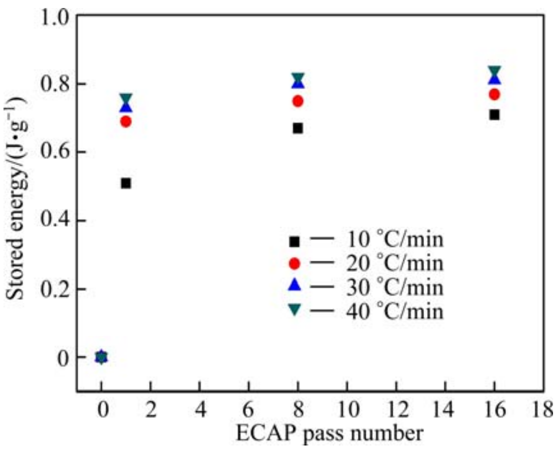

Fig. 3 Evolution of stored energy of Cu−1Cr−0.1Zr alloy versus ECAP pass number

Our findings are in good agreement with those of HIGUERA-COBOS and CABRERA [33] who found that the stored energy depended on the heating rate and at the higher rates (20 and 40 °C/min), the differences between the curves were very weak. HIGUERA-COBOS and CABRERA[33] and SCHAFLER et al [34] considered that individual defects components may contribute to the total signal. Dislocations and vacancies are the most probable defects that can be detected during calorimetry measurements. SETMAN et al [35] evidenced the contribution of both defects with the presence of not only single/double vacancies but also vacancy agglomerates as well in pure Ni, while in SPD-processed Cu, only vacancy agglomerates were presented with dislocations. The specific single/double vacancy peak was not evidenced in the present work for any DSC scan for all the heating rates, demonstrating that Cu−1Cr−0.1Zr alloy subjected to 1, 4, 8 and 16 ECAP passes behaved like pure Cu.

Figure 4 presents the Kissinger plots for recrystallization peaks measured by DSC for Cu−1Cr−0.1Zr alloy after ECAP processing. The deduced activation enthalpy values are −135.8, −137.4 and 117.12 kJ/mol respectively for 1, 8 and 16 ECAP passes. For 1 and 16 passes, the curves linear fits to the experimental points are very close to one another, while that for 8 passes slightly separates from them. Almost all values of activation enthalpy are a little higher than those tabulated in the literature for existing data for Cu [33,34,36,37]. As discussed by HIGUERA-COBOS and CABRERA [33], the higher value of activation energy for the first pass may be caused by the large proportion of subgrains, while for the higher pass numbers, the trends are reversed and the processes of recovery of the microstructure may be generated with a considerable fraction of high angle grain bounadries. Usually, for pure Cu, the activation enthalpy values range between 0.67 to 1.3 Ev, indicating that recrystallization takes place by a mechanism of migration of high angle grain boundaries [33,34,36,37]. In the present work, a strong influence of the complex precipitation process should delay the recrystallization, and the precipitating particles influence both the rearrangement of dislocations to form recrystallization fronts and the migration of the latter as discussed by HORNBOGEN and KÖSTER [38].

Figure 5 presents the the dislocation density for Cu−1Cr−0.1Zr alloy as a function of number of ECAP passes deduced from stored energy measured by DSC and using Eq. (3) given by [32,39]

$$E_{st} = Gb^2 \frac{N}{4\pi k}(b\sqrt{N})^{-1} \tag{3}$$

where G is the shear modulus and b is the absolute value

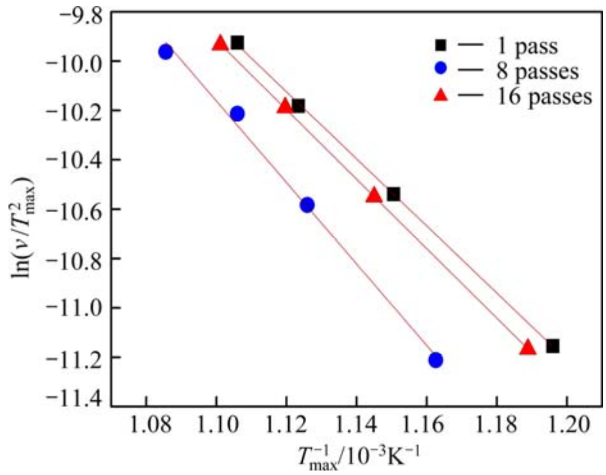

Fig. 4 Kissinger plots for recrystallization peaks measured by DSC for Cu−1Cr−0.1Zr alloy (Experimental points data are fitted by full lines)

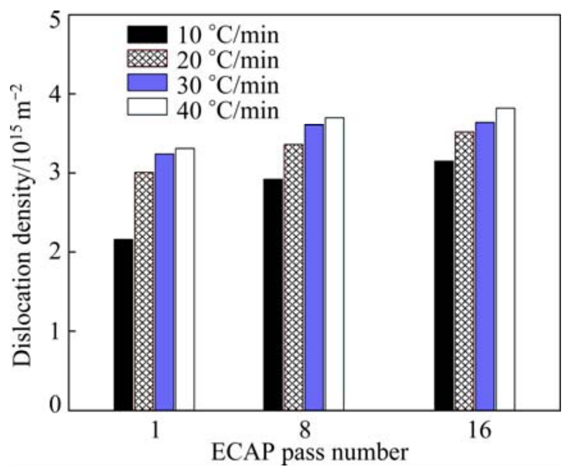

Fig. 5 Dislocation density as a function of number of ECAP passes deduced from stored energy measured by DSC for Cu−1Cr−0.1Zr alloy

of Burgers vector, k is an arithmeatic average of 1 and $(1-\upsilon)$ with υ=0.343 being the Poisson ratio for Cu. Quasi parabolic evolution of the dislocation density versus the ECAP number pass is noticed however without any saturation as observed for pure Cu [33]. HIGUERA-COBOS and CABRERA [33] demonstrated that dislocation density versus the ECAP number passes was in good correlation with electrical conductivity, and one can conlude from Fig. 6 that the addition of Cr and Zr does not significantly affect this correlation. Furthermore, our results are in line with several investigations that have shown that the electrical conductivity of Cu-based materials decreased upon increasing strain [40,41].

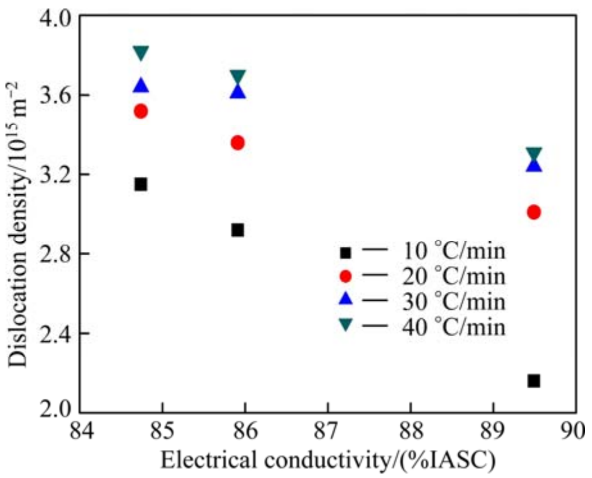

Fig. 6 Correlation of dislocation density with electrical conductivity of Cu−1Cr−0.12Zr alloy as a function of heating rate

4 Conclusions

1) Samples of commercial Cu−1Cr−0.1Zr alloy (CRZ copper) are subjected to equal channel angular pressing (ECAP) up to 16 passes at room temperature following route B_c.

2) The sequence of precipitation consists firstly on the Cr clustering followed by the nano precipitation of $Cu_{51}Zr_{14}$ phase with activation energy in the ranges of 121−142 and 131−181 kJ/mol, respectively. The deduced activation enthalpy of recrystallization is in the range of from −117 to −137 kJ/mol.

3) The recrystallization temperatures decrease while the stored energy increases with increasing strain. A saturation of the stored energy of 0.7−0.8 J/g is noticed. The deduced dislocation density from the stored energy versus the ECAP number passes is in good correlation with electrical conductivity.

Acknowledgements

The authors wish to heartily thank Pr. Jose Maria CABRERA from Polytecnia ETSEIB, Universidad Politécnica de Cataluña, for inviting and helping Miss K. ABIB during her several scientific stays and Dr. Ana HERNANDEZ from Fundació CTM Centre Tecnològic, Av. de les Bases de Manresa (Barcelona), Cataluña, for her kind assistance during DSC measurements. Dr. Hiba AZZEDDINE from M'sila University, Algeria, is heartily acknowledged for the manuscript improvement.

References

[1] EDWARDS D J, SINGH B N, TÄHTINEN S. Effect of heat treatments on precipitate microstructure and mechanical properties of a CuCrZr alloy [J]. J Nucl Mater, 2007, 367−370: 904−909.

[2] HUANG F, JUSHENG M, HONGONG N, ZHITING G, LU C, SHUMEI G, YU X T, TAO W, LI H, HUAFEN L. Analysis of phases in a Cu−Cr−Zr alloy [J] Scripta Mater, 2003, 48(1): 97−012.

[3] WANG Zhi-qiang, ZHONG Yun-bo, RAO Xian-jun, WANG Chao, WANG Jiang, ZHANG Zeng-guang, REN Wei-li, REN Zhong-ming. Electrical and mechanical properties of Cu−Cr−Zr alloy aged under imposed direct continuous current [J]. Transactions of Nonferrous Metals Society of China, 2012, 22(5): 1106−1111.

[4] MUGHRABI H. On the grain-size dependence of metal fatigue: Outlook on the fatigue of ultrafine-grained metals [M]// Investigations and Applications of Severe Plastic Deformation, Vol.80, Nato Science Series. Kluwer, 2000: 241−253.

[5] VINOGRADOV A, PATLAN V, SUZUKI Y, KITAGAWA K, KOPYLOV V I. Structure and properties of ultra-fine grain Cu−Cr−Zr alloy produced by equal-channel angular pressing [J]. Acta Mater, 2002, 50(7): 1639−1651.

[6] GAO N, STARINK M J, LANGDON T G. Using differential scanning calorimetry as an analytical tool for ultrafine grained metals processed by severe plastic deformation [J]. J Mater Sci Technol, 2009, 25: 687−698.

[7] VALDÈS LEÓN K, MUŇOZ-MORRIS M A, MORRIS D G. Optimization of strength and ductility of a Cu−Cr−Zr alloy by combination of severe plastic deformation and precipitation [J]. Mater Sci Eng A, 2012, 536: 181−189.

[8] MUŇOZ-MORRIS M A, VALDÈS LEÓN K, CABALLERO F G, MORRIS D G. A study of changes taking place in Cu−Cr−Zr alloy during severe plastic deformation and annealing as evaluated by thermoelectric power measurements [J]. Scripta Mater, 2012, 67: 806−809.

[9] KISSINGER H E. Reaction kinetics in differential thermal analysis [J]. Anal Chem, 1957, 29 (11): 1702−1706.

[10] GIANNOZZI P, BARONI S, BONINI N, CALANDRA M, CAR R, CAVAZZONI C, CERESOLI D, CHIAROTTI GL, COCOCCIONI M, DABO I, DAL CORSO A, FABRIS S, FRATESI G, GIRONCOLI S, GEBAUER R, GERSTMANN U, GOUGOUSSIS C, KOKALJ A, LAZZERI M, MARTIN-SAMOS L, MARZARI N, MAURI F, MAZZARELLO R, PAOLINI S, PASQUARELLO A, PAULATTO L, SBRACCIA C, SCANDOLO S, SCLAUZERO G, SEITSONEN A P, SMOGUNOV A, UMARI P, WENTZCOVITCH R M. Quantum espresso: A modular and open-source software project for quantum simulations of materials [J]. J Phys Condense Matter, 2009, 21: 395502.

[11] HOHENBERG P, KOHN W. Inhomogeneous electron gas [J]. Physical Review B, 1964, 136(3): 864−871.

[12] KOHN W, SHAM L J. Self-consistent equations including exchange and correlation effects [J]. Physical Review A, 1965, 140(4): 1133−1138.

[13] PREDEW J P, BURKE K, ERNZERHOF M. Generalized gradient approximation made simple [J]. Phys Rev Lett, 1996, 77(18): 3865−3868.

[14] VANDERBILT D. Soft self-consistent pseudopotentials in a

generalized eigenvalue formalism [J]. Physical Review B, 1990, 41(11): 7892−7895.

[15] FISHER T H, ALMLOF J. General methods for geometry and wave function optimization [J]. J Phys Chem, 1992, 96(24): 9768−9774.

[16] HOLZWARTH U, STAMM H. The precipitation behaviour of ITER-grade Cu−Cr−Zr alloy after simulating the thermal cycle of hot isostatic pressing [J]. J Nucl Mater, 2000, 279: 31−45.

[17] WANG J, IWAHASHI Y, HORITA Z, FURUKAWA M, NEMOTO M, VALIEV R Z, LANGDON T G. An investigation of microstructural stability in an Al−Mg alloy with submicrometer grain size [J]. Acta Mater, 1996, 44(7): 2973−2982.

[18] AZZEDDINE H, MEHDI B, HENNET L, THIAUDIÈRE D, ALILI B, KAWASAKI M, BRADAI D, LANGDON T G. An in situ synchrotron X-ray diffraction study of precipitation kinetics in a severely deformed Cu−Ni−Si alloy [J]. Mater Sci Eng A, 2014, 597(12): 288−294.

[19] ANGELLA G, BASSANI P, TUISSI A, RIPAMONTI D, VEDANI M. Microstructure evolution and aging kinetics of Al−Mg−Si and Al−Mg−Si−Sc alloys processed by ECAP [J]. Mater Sci Forum, 2006, 503−504: 439−446.

[20] KIM W J, WANG J Y. Microstructure of the post-ECAP aging processed 6061 Al alloys [J]. Mater Sci Eng A, 2007, 464(1−2): 23−27.

[21] SU J, LIU P, REN, DONG Q. Phase transformation in Cu−Cr−Zr−Mg alloy [J]. Mater Lett, 2007, 61: 4963−4966.

[22] MORRIS M A, LEBOEUF M, MORRIS D G. Recrystallization mechanisms in a Cu−Cr−Zr alloy with a bimodal distribution of particles [J]. Mater Sci Eng A, 1994, 188(1−2): 255−265.

[23] ROHRER G S. Introduction to grains, phases, and interfaces—An interpretation of microstructure [J]. Metall Mater Trans A, 2010, 41: 1063−1100.

[24] SUN Z, GUO J, SONG X, ZHU Y, LI Y. Effects of Zr addition on the liquid phase separation and the microstructures of Cu−Cr ribbons with 18−22 at.% Cr [J]. J Alloys Compd, 2008, 455(1−2): 243−248.

[25] GOSH G. First principles calculations of structural energetic of Cu−TM (TM=Ti, Zr, Hf) intermetallics [J]. Acta Mater, 2007, 55(10): 3347−3374.

[26] ARIAS D, ABRIATA J P. Cu−Zr (Copper−Zirconium) [J]. Bull Alloy Phase Diagrams, 1990, 11: 452−459.

[27] ARIAS D, ABRIATA J P. Cu−Zr (Copper−Zirconium) [M]//Phase Diagrams of Binary Copper Alloys. ASM Materials Park, OH, 1994: 497−502.

[28] SHEIBANI S, HESHMATI-MANESH S, ATAIE A, CABALLERO A, CRIADO J M. Spinodal decomposition and precipitation in Cu−Cr nanocomposite [J]. J Alloys Compd, 2014, 587: 670−676.

[29] DONOSO E, ESPINOZA R, DIANEZ M J, CRIADO J M. Microcalorimetric study of the annealing hardening mechanism of a Cu−2.8Ni−1.4Si (at%) alloy [J]. Mater Sci Eng A, 2012, 556: 612−616.

[30] VARSCHAVSKY A, DONOSO E. A differential scanning calorimetric study of precipitation in Cu−2Be [J]. Thermochim Acta, 1995, 266: 257−275.

[31] HADJ LARBI F, ABIB K, KHEREDDINE Y, ALILI B, KAWASAKI M, BRADAI D, LANGDON T G. DSC analysis of an ECAP-deformed Cu−Ni−Si alloy [C]//Proceedings of the 22nd International Conference on Metallurgy and Materials (Metal’2013). Brno, Czech Republic, EU, 2013.

[32] CAO Q, GU C F, PERELOMA E V, DAVIES C H J. Stored energy, vacancies and thermal stability of ultra-fine grained copper [J]. Mater Sci Eng A, 2008, 492: 74−79.

[33] HIGUERA-COBOS O F, CABRERA J M. Mechanical, microstructural and electrical evolution of commercially pure copper processed by equal channel angular extrusion [J]. Mater Sci Eng A, 2013, 571: 103−114.

[34] SCHAFLER E, STEINER G, KORZNIKOVA E, KERBER M, ZEHETBAUER M J. Lattice defect investigation of ECAP-Cu by means of X-ray line profile analysis, calorimetry and electrical resistometry [J]. Mater Sci Eng A, 2005, 410−411: 169−173.

[35] SETMAN D, SCHAFLER E, KORZNIKOVA E, ZEHETBAUER M J. The presence and nature of vacancy type defects in nanometals detained by severe plastic deformation [J]. Mater Sci Eng A, 2008, 493: 116−122.

[36] MOLODOVA X, GOTTSTEIN G, WINNING M, HELLMIG R J. Thermal stability of ECAP processed pure copper [J]. Mater Sci Eng A, 2007, 460−461: 204−213.

[37] VISWANATHAN R, BAUER C L. Kinetics of grain boundary migration in copper bicrystals with [001] rotation axes [J]. Acta Metall, 1973, 21(8): 1099−1109.

[38] HORNBOGEN E, KÖSTER E. Recrystallization of two-phase alloy [M]//Frank HAESSNER, Recrystallization of Metallic Materials. Stuttgart: Rieder Verlag GmbH, 1978: 159−194.

[39] IWAHASHI Y, HORITA Z, NEMOTO M, LANGDON T G. An investigation of microstructural evolution during equal-channel angular pressing [J]. Acta Mater, 1997, 45: 4733−4741.

[40] HOSSEINI S A, MANESH H D. High-strength, high-conductivity ultra-fine grains commercial pure copper produced by ARB process [J]. Mater Des, 2009, 30: 2911−2918.

[41] ÇETINARSLAN C S. Effect of cold plastic deformation on electrical conductivity of various materials [J]. Mater Des, 2009, 30: 671−673.

等径转角挤压 Cu−Cr−Zr 合金的差热分析

K. ABIB, F. HADJ LARBI, L. RABAHI, B. ALILI, D. BRADAI

Faculty of Physics, University of Sciences and Technology Houari Boumediene,
BP 32 El Alia, Bab Ezzouar, Algiers, Algeria

摘　要：对 Cu−1Cr−0.1Zr 合金在室温下进行 16 道次等径转角挤压(ECAP)，挤压路径为 B_c。利用差热分析研究合金中沉淀相的析出序列，计算每道次 ECAP 后合金储能、再结晶温度以及激活能。此外，对位错密度与电学性能之间的关系进行研究。结果表明：随着 ECAP 挤压道次的增加，合金中的储能增加，而再结晶温度则大幅度降低。

关键词：等径转角挤压；Cu−Cr−Zr 合金，差热分析；电导率；储能

(Edited by Yun-bin HE)